ChemPubSoc Europe

DOI: 10.1002/chem.201901499

CHEMISTRY
A European Journal
Communication

Graphene Oxide

Brodie's or Hummers' Method: Oxidation Conditions Determine the Structure of Graphene Oxide

Patrick Feicht,*[a] Johannes Biskupek,[b] Tatiana E. Gorelik,[b] Julian Renner,[b] Christian E. Halbig,[a] Maria Maranska,[a] Florian Puchtler,[c] Ute Kaiser,[b] and Siegfried Eigler*[a]

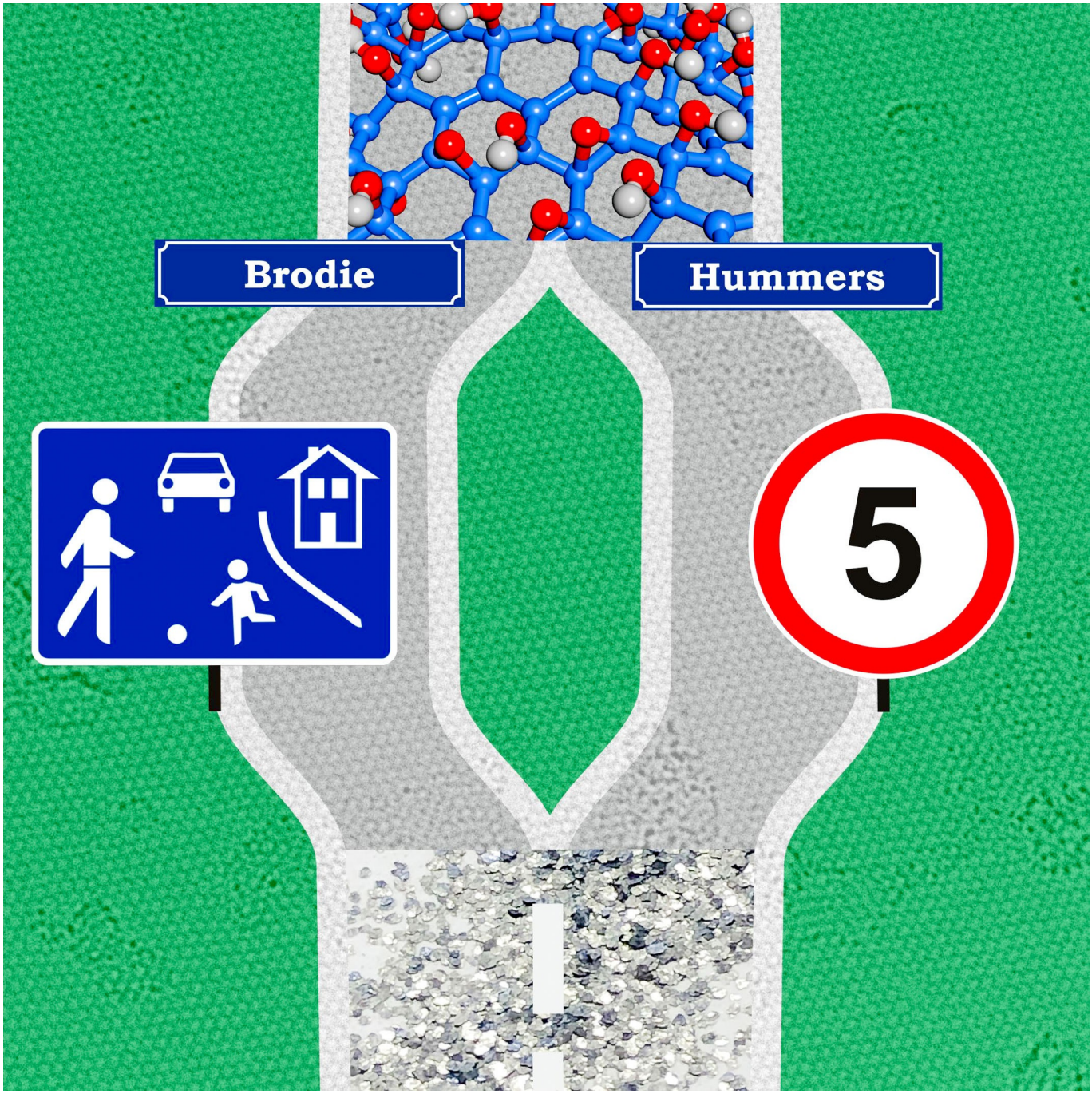

Abstract: Synthesis and studies of graphite oxide started more than 150 years ago and turned into a boom by the measurements of the outstanding physical properties of graphene. A series of preparation protocols emanated trying to optimize the synthesis of graphene oxide in order to obtain a less defective material, as source for graphene. However, over-oxidation of the carbon framework hampered establishing structure-property relationships. Here, the fact that two different synthetic methods for graphene oxide preparation lead to very similar types of graphene oxide with a preserved graphene lattice is demonstrated. Either sodium chlorate in nitric acid (similar to Brodie's method) or potassium permanganate in sulfuric acid (similar to Hummers' method) treatment are possible; however, reaction conditions must be controlled. With a preserved carbon lattice analytical differences between the samples relate to the altered on-plane functionality. Consequently, terming preparation protocols "according to Brodie's/Hummers' method" is not sufficient.

The scalable preparation of graphene from water-dispersed precursors remains difficult because the quality of the produced graphene is usually very low and it is highly heterogeneous.[1] Oxidation of graphite facilitates delamination by addition of oxo-addends to the graphene lattice to overcome the attractive van der Waals forces. Thus, water-insoluble graphite is transformed into water-dispersible graphene oxide (GO). However, over-oxidation leads to a ruptured carbon-framework and consequently an amorphous carbon lattice. The oxidation process has been studied for over the last 150 years by many pioneers in GO research, namely Schafhaeutl,[2] Brodie,[3] Luzi,[4] Staudenmaier,[5] Charpy,[6] Kohlschütter,[7] Haenni,[7] Thiele,[8] Hofmann,[9] Frenzel,[10] Scholz,[11] Boehm,[12] Hummers and Offeman.[13] All protocols have in common that a concentrated strong acid is used along with an oxidizing agent, or electrochemical oxidation is applied.[14] However, GOs with undefined concentrations of lattice defects and different degrees and types of functionalization are obtained by those protocols, making structure evaluation illusive.

Research on GO turned however into an outstanding impact. The publication "*Preparation of Graphitic Oxide*" by William S. Hummers Jr. and Richard E. Offeman in 1958[13] has attracted the scientific attention in recent years, which is reflected in >18000 citations recorded on Scopus. The described method is termed Hummers' method, or modified Hummers' method, when graphite is pretreated.[15]

A series of other oxidizing agents have been tested, such as Ce^{IV}, Co^{III}, NaOCl, $(NH_4)_2S_2O_8$ and OsO_4.[16] However, only two methods lead to an utterly formation of GO and are therefore mainly used. The first method has been described by Brodie in 1859.[3] Fuming nitric acid is dropped onto a physical mixture of graphite and sodium chlorate at which only small amounts of the oxidant are formed in situ. Delamination is only triggered by the addition of a base for the deprotonation of less acidic functional groups. For the second method, described by Hummers and Offeman, potassium permanganate dissolved in sulfuric acid is used to oxidize the graphite dispersed therein.[13] This GO spontaneously delaminates by osmotic swelling in water even at low pH values due to a highly negative surface potential in particular caused by organosulfates.[17]

Harsh reaction conditions usually lead to materials with different physical properties[18] and a distorted carbon lattice due to over-oxidation.[1] However, we demonstrated that by controlling the temperature of the reaction the carbon framework could be preserved.[19] This low-defect type of GO, which we term oxo-functionalized graphene (oxo-G), can be converted back to graphene by reductive defunctionalization.[19] As a consequence of a preserved carbon lattice the on-plane chemistry could be studied.[20] Nevertheless, the question remains, whether other methods can also prevent over-oxidation of the carbon lattice. If so, properties could for the first time be clearly related to the altered on-plane chemistry.

Here, we show that the oxidation of graphite by sodium chlorate in fuming nitric acid can also be used to prepare GO with a highly intact graphene lattice. The used protocol is very similar to that published by Brodie.[3] We conclude that, although different acids with different oxidants are used, the products prepared are part of the same class of oxo-functionalized graphene materials, with oxo-addends attached to the hexagonal carbon lattice and a predominantly preserved carbon lattice. This observation allows for the unification of the preparation methods of oxo-G for the first time and renders the understanding of the class of GO no longer elusive.

At first, oxo-G^{ref} was synthesized according to our previously published protocol as the reference material (Figure 1).[19] Accordingly, graphite was dispersed in cold sulfuric acid (<10 °C) and potassium permanganate was slowly added. The workup procedure was accomplished by slow continuous addition of water and hydrogen peroxide, also keeping the temperature below 10 °C, thereby controlling the microkinetics. Upon washing the ionic strength is reduced, which triggers delamination of this oxo-G by osmotic swelling. In addition, oxo-$G^{4\%}$ was synthesized from the intercalation compound graphite sulfate and aqueous treatment.[21] Oxo-$G^{4\%}$ possesses, to a first approximation, 4% of hydroxyl addends related to the number of C atoms.[21,22] Moreover, over-oxidized graphene oxide (GO^{st}) was prepared as described in the literature.[13]

The oxidation protocol, according to Brodie, involves successive oxidation steps of graphite.[3] In each step, fuming nitric

[a] *Dr. P. Feicht, Dr. C. E. Halbig, M. Maranska, Prof. Dr. S. Eigler*
Institute of Chemistry and Biochemistry, Freie Universität Berlin
Takustraße 3, 14195 Berlin (Germany)
E-mail: patrick.feicht@fu-berlin.de
siegfried.eigler@fu-berlin.de

[b] *Dr. J. Biskupek, Dr. T. E. Gorelik, J. Renner, Prof. Dr. U. Kaiser*
Materialwissenschaftlische Elektronenmikroskopie, Universität Ulm
Albert-Einstein-Allee 11, 89081 Ulm (Germany)

[c] *F. Puchtler*
Lehrstuhl für Anorganische Chemie I, Universität Bayreuth
Universitätsstraße 30, 95440 Bayreuth (Germany)

Supporting information and the ORCID identification number(s) for the author(s) of this article can be found under:
https://doi.org/10.1002/chem.201901499.

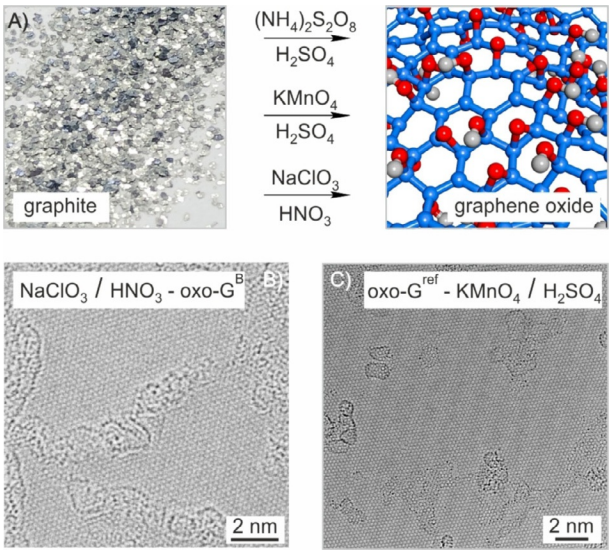

Figure 1. A) Reaction scheme of the oxidation of graphite by different protocols, all leading to oxo-addends attached to the hexagonal carbon lattice, termed either graphene oxide or oxo-functionalized graphene. B) and C) −80 kV HRTEM images acquired with the C_C/C_S-corrected SALVE instrument at atomic resolution depicting the hexagonal carbon lattice of graphene (and amorphous carbon impurities) after the oxidation of graphite by sodium chlorate in nitric acid and potassium permanganate in sulfuric acid, respectively.

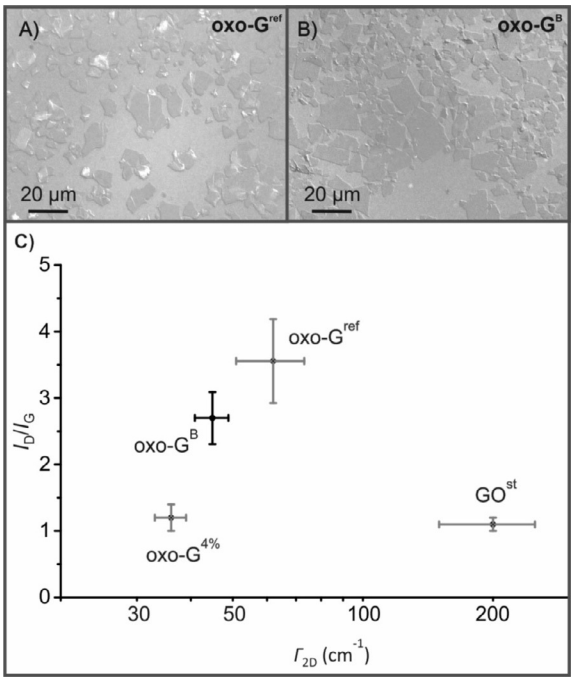

Figure 2. Optical microscope images (differential interference contrast) of films of flakes on Si/300 nm SiO_2 substrates of A) oxo-G^{ref} and B) oxo-G^B. C) Plot of the statistical Raman spectroscopy data of oxo-G samples prepared by different oxidation protocols. Samples oxo-G^{ref}, oxo-$G^{4\%}$, oxo-G^B and GO^{st} are compared.

acid is dropped onto a mixture of graphite and potassium chlorate. Thereafter, the reaction mixture is allowed to react overnight and is then slowly heated to 60 °C for the evaporation of excess nitric acid. The reaction can be safely performed in an open vessel preventing accumulation of evolving ClO_2 (caution: accumulation of ClO_2 may lead to explosive decomposition). Control of the oxidation and preventing over-oxidation of the carbon lattice is achieved by macrokinetic control of solid/liquid/gas phase interaction of gaseous ClO_2 in nitric acid and graphite. The oxidation was repeated three times to synthesize oxo-G^B. Single layers were obtained after delamination and probed (Figure 1 and Figure 2). The yield of delaminable material exceeds 95%. Films of flakes were prepared by using the Langmuir–Blodgett technique and optical microscope images are depicted in Figure 2A,B. In addition, AFM images corroborate the delamination of oxo-G^B into single layers with a measured height of about 1 nm (Figure S1, Supporting Information).

Statistical Raman spectroscopy (SRS) of graphene allows for the determination of the density of in-plane vacancy defects of graphene.[23] Therefore, the samples were reduced by hydroiodic acid prior to measuring Raman spectra. For all samples the $I_D/I_{D'}$ ratio was about 7, indicating mainly vacancy defects and confirming a thorough defunctionalization by reduction.[24] It is evident from the broad 2D band with a full width at half maximum (Γ_{2D}) of around 200 cm^{-1} (Figure 2) that GO^{st} possesses extended defects.[25] In contrast, for oxo-G^B the average Γ_{2D} values are approximately 44 cm^{-1} (Figure 2) with an average I_D/I_G ratio of 2.7. The corresponding density of defects for oxo-G^B is about 0.07%. Such values indicate that the carbon framework remains almost intact,[23a,26] which can be corroborated as visualized in Figure 1B by using transmission electron microscopy at atomic resolution.

Consequently, mainly functionalization of the graphene lattice takes place. With each oxidation step, only a vanishing amount of vacancy defects is introduced. The density of defects for the reference samples oxo-$G^{4\%}$ and oxo-G^{ref} are 0.02% and 0.5%, respectively.

Aberration-corrected high-resolution transmission electron microscopy (AC-HRTEM) investigation provides direct probing of the exceptional integrity of the carbon frameworks after gentle electron-beam induced release of oxo-functionalities, for both oxo-G^B and oxo-G^{ref}, as depicted in Figure 1B,C. Moreover, Fourier-transformation of the HRTEM images reveal a hexagonal pattern confirming a long-range order of the graphene lattice (Figures S2–S14, Supporting Information). The amorphous coverages on the surface are attributed to unspecified adsorbates from sample preparation under ambient conditions. Consequently, the carbon framework of oxo-G^B is similar to oxo-G^{ref} (Figure 1C, Figures S15 and S16 in the Supporting Information).

Moreover, the high sensitivity of X-ray diffraction to changes in crystallinity allows for a well-defined analysis of the structural integrity. The 001 reflection at 13.75° in the diffraction pattern of oxo-G^B corresponds to an interlayer distance of 0.64 nm and it is in accordance with literature values (Figure 3).[27] In contrast, the interlayer distance of oxo-G^{ref} is 0.86 nm, due to the bulky organosulfate groups and physisorbed water (Figure S17, Supporting Information).

The broadening of this peak and the cancellation of the rest of the 00*l* series is due to a turbostratic ordering of the plate-

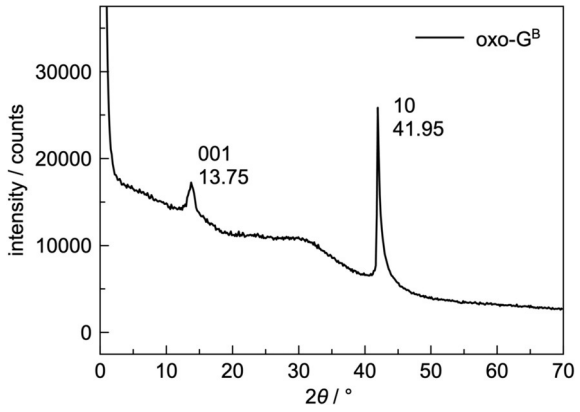

Figure 3. X-ray diffraction pattern of oxo-G^B.

lets, which is also the cause for the lambda shape of the hk band at 41.95°.[28] The hk band provides information about the periodic arrangement of the atoms within the hexagonal lattice. The sharp 10 band of a high intensity therefore corresponds to an exceptionally high integrity of the graphene lattice and is unprecedented up to now. An eightfold higher concentration of defects as in oxo-G^{ref} results in a nearly complete cancellation of this band (Figure S17, Supporting Information).

As evident from the combustion elemental analyses of oxo-G derivatives (bulk analysis), the lowest C content was found for oxo-G^{ref} with a mass content of about 43%. However, this value needs to be corrected in order to compare it to oxo-G^B. Oxo-G^{ref} bears about one organosulfate group with a hydronium ion as counterion on 17 C atoms (Table 1), as we have described in detail before.[17b] Considering that one sulfur atom of organosulfate in oxo-G^{ref} is bound to four oxygen atoms and one hydronium ion,[17b] a C content of 57% would be expected, if organosulfate and the counterion were cleaved (oxo-$G^{ref\text{-}S}$). Consequently, the degree of oxidation is very similar for oxo-G^{ref} and oxo-G^B. In contrast, for oxo-$G_{4\%}$ the degree of functionalization is only about 4%,[21,22,29] and consequently a C content of about 86% is found.

Table 1. Combustion elemental analysis data of oxo-G^{ref}, oxo-$G^{ref\text{-}S}$, oxo-$G_{4\%}$, and oxo-G^B.

	C [%]	H [%]	N [%]	S [%]	O [%] calcd
oxo-G^{ref}	43.36	2.29	–	6.67	47.68
oxo-$G^{ref\text{-}S}$	57.17	2.16	–	corrected (-OSO_3H_3O)	40.67
oxo-$G_{4\%}$	85.72	1.01	–	1.59	11.68
oxo-G^B	59.97	1.70	0.30	–	38.03

In addition, nuclear magnetic resonance spectra recorded in the solid state (ssNMR) basically show four signals for oxo-G^{ref} and oxo-G^B (Figure 4). At around 59 ppm, the signal of epoxy groups resonates and at about 69–70 ppm the signal for hydroxyl groups is found. At 129–135 ppm signals from sp^2 carbon atoms are found, in particular sp^2 carbon atoms in proximity to epoxy groups (129–130 ppm) and hydroxyl groups (133–135 ppm), respectively.[30] To a first approximation,

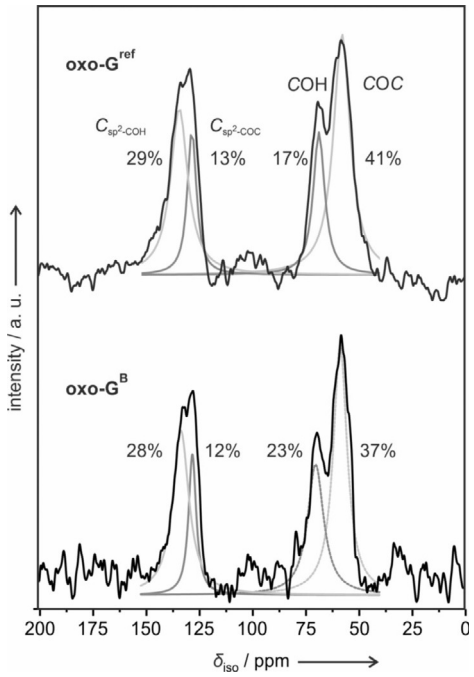

Figure 4. Nuclear magnetic resonance spectra measured in solids of oxo-G^{ref} and oxo-G^B.

about 60% sp^3 carbon is found for oxo-G^{ref} and oxo-G^B, respectively, and the ratio of hydroxyl to epoxy groups is roughly 1:1 (taking into account that the oxygen in the epoxy group is bound to two carbon atoms).

Consequently, according to the quantitative bulk analysis, the only major difference between oxo-G^{ref} and oxo-G^B is that oxo-G^{ref} bears organosulfate groups as a consequence of esterification of hydroxyl groups in sulfuric acid. In contrast, FTIR spectra of oxo-G^B compared to oxo-G^{ref} appears to be complex, possibly due to the combination of vibrational modes (Figure S18, Supporting Information). With the finding that the carbon framework of both oxo-G^{ref} and oxo-G^B are intact it is plausible to attribute the differences in delamination behavior to organosulfate groups, which facilitate delamination in water for oxo-G^{ref}, whereas oxo-G^B needs some base treatment for efficient delamination.

With the synthesis of GO by Brodie's method and proving the integrity of the carbon framework, the mystery of different methods for the synthesis of graphene oxide is more clarified. Moreover, it is no longer elusive to determine structural properties of derivatives of GO. Preservation of an intact carbon lattice of graphene and quantification of the residual density of vacancy defects is, however, the basis to interpret spectroscopic details.

The main differences between the produced oxo-G materials are related to the degree of functionalization and elemental analysis, thermogravimetric analysis and ssNMR spectroscopy give information about major functional groups. In addition, another difference between oxo-G^{ref} and oxo-G^B is that oxo-G^B is a priori free from manganese ions and sulfur species. Those must be removed from oxo-G^{ref} by washing procedures using HCl.[31] The knowledge about minor impurities is important, for

example, for cell applications, considering that the toxicity depends on minor impurities and minor amounts of endoperoxides, or studies of catalytic activities, given that manganese species may be catalytically active.[31]

In summary, we have demonstrated that different oxidation procedures can lead to oxo-G derivatives with the same highly intact carbon lattice by controlling either the micro- or macrokinetics. This strengthens the need for the chemical analysis of GO used in applications. We confirmed that oxidation protocols, similar to those introduced by Brodie or Hummers and Offeman, can lead to GO with an intact carbon framework, which was not confirmed for the oxidation of graphite by sodium chlorate in nitric acid before. These finding paves the way to explore the full potential of oxo-G in high-tech applications in which the exceptional properties of a throughout intact graphene lattice are essential, such as electronic devices, thermally conductive materials, reinforcing filler in polymer nanocomposites or gas barriers. Controlling the presence of minor species, such as metal impurities, carbon-centered radicals or endoperoxide groups,[31] is important to facilitate applications in biological systems.[32] However, our finding moreover gives access to control the on-plane regiochemistry of oxo-G and graphene, respectively, bearing assumedly a high potential for advancing applications.[33]

Acknowledgements

This research was funded by the Deutsche Forschungsgemeinschaft (DFG, German Research Foundation, project number 392444269, CRC1279), the BioSupraMol core facility and by the DFG and the Land Baden–Württemberg in the frame of the SALVE project. P.F. thanks Tamás Szabó for giving very helpful advice regarding the GO synthesis according to Brodie's method. We thank Prof. Josef Breu for access to the XRD equipment.

Conflict of interest

The authors declare no conflict of interest.

Keywords: graphene · graphene oxide · oxo-functionalized graphene · spectroscopy

[1] P. Feicht, R. Siegel, H. Thurn, J. W. Neubauer, M. Seuss, T. Szabo, A. V. Talyzin, C. E. Halbig, S. Eigler, D. A. Kunz, A. Fery, G. Papastavrou, J. Senker, J. Breu, *Carbon* **2017**, *114*, 700.
[2] C. Schafhaeutl, *J. Prakt. Chem.* **1840**, *21*, 129.
[3] B. C. Brodie, *Philos. Trans. R. Soc. London* **1859**, *149*, 249.
[4] W. Luzi, *Z. Naturwiss.* **1891**, *64*, 224.
[5] L. Staudenmaier, *Ber. Dtsch. Chem. Ges.* **1898**, *31*, 1481.
[6] G. Charpy, *C. R. Acad. Sci.* **1909**, *148*, 920.
[7] V. Kohlschütter, P. Haenni, *Z. Anorg. Allg. Chem.* **1919**, *105*, 121.
[8] H. Thiele, *Z. Anorg. Allg. Chem.* **1930**, *190*, 145.
[9] U. Hofmann, *Ber. Dtsch. Chem. Ges.* **1928**, *61*, 435.
[10] U. Hofmann, A. Frenzel, *Ber. Dtsch. Chem. Ges.* **1930**, *63*, 1248.
[11] A. Clause, R. Plass, H. P. Boehm, U. Hofmann, *Z. Anorg. Allg. Chem.* **1957**, *291*, 205.
[12] W. Scholz, H. P. Boehm, *Z. Anorg. Allg. Chem.* **1969**, *369*, 327.
[13] W. S. Hummers, R. E. Offeman, *J. Am. Chem. Soc.* **1958**, *80*, 1339.
[14] H. Thiele, *Z. Elektrochem.* **1934**, *40*, 26.
[15] N. I. Kovtyukhova, P. J. Ollivier, B. R. Martin, T. E. Mallouk, S. A. Chizhik, E. V. Buzaneva, A. D. Gorchinskiy, *Chem. Mater.* **1999**, *11*, 771.
[16] H. P. Boehm, M. Eckel, W. Scholz, *Z. Anorg. Allg. Chem.* **1967**, *353*, 236.
[17] a) P. Feicht, D. A. Kunz, A. Lerf, J. Breu, *Carbon* **2014**, *80*, 229; b) S. Eigler, C. Dotzer, F. Hof, W. Bauer, A. Hirsch, *Chem. Eur. J.* **2013**, *19*, 9490.
[18] a) S. You, S. M. Luzan, T. Szabó, A. V. Talyzin, *Carbon* **2013**, *52*, 171; b) A. V. Talyzin, A. Klechikov, M. Korobov, A. T. Rebrikova, N. V. Avramenko, M. F. Gholami, N. Severin, J. P. Rabe, *Nanoscale* **2015**, *7*, 12625; c) M. V. Korobov, A. V. Talyzin, A. T. Rebrikova, E. A. Shilayeva, N. V. Avramenko, A. N. Gagarin, N. B. Ferapontov, *Carbon* **2016**, *102*, 297.
[19] S. Eigler, M. Enzelberger-Heim, S. Grimm, P. Hofmann, W. Kroener, A. Geworski, C. Dotzer, M. Rockert, J. Xiao, C. Papp, O. Lytken, H. P. Steinrück, P. Müller, A. Hirsch, *Adv. Mater.* **2013**, *25*, 3583.
[20] S. Eigler, *Chem. Eur. J.* **2016**, *22*, 7012.
[21] S. Seiler, C. E. Halbig, F. Grote, P. Rietsch, F. Borrnert, U. Kaiser, B. Meyer, S. Eigler, *Nat. Commun.* **2018**, *9*, 836.
[22] S. Eigler, *Chem. Commun.* **2015**, *51*, 3162.
[23] a) M. M. Lucchese, F. Stavale, E. H. M. Ferreira, C. Vilani, M. V. O. Moutinho, R. B. Capaz, C. A. Achete, A. Jorio, *Carbon* **2010**, *48*, 1592; b) L. G. Cançado, A. Jorio, E. H. Ferreira, F. Stavale, C. A. Achete, R. B. Capaz, M. V. Moutinho, A. Lombardo, T. S. Kulmala, A. C. Ferrari, *Nano Lett.* **2011**, *11*, 3190; c) S. Eigler, F. Hof, M. Enzelberger-Heim, S. Grimm, P. Muller, A. Hirsch, *J. Phys. Chem. C* **2014**, *118*, 7698.
[24] A. Eckmann, A. Felten, A. Mishchenko, L. Britnell, R. Krupke, K. S. Novoselov, C. Casiraghi, *Nano Lett.* **2012**, *12*, 3925.
[25] S. Eigler, C. Dotzer, A. Hirsch, *Carbon* **2012**, *50*, 3666.
[26] L. G. Cançado, A. Jorio, E. H. M. Ferreira, F. Stavale, C. A. Achete, R. B. Capaz, M. V. O. Moutinho, A. Lombardo, T. S. Kulmala, A. C. Ferrari, *Nano Lett.* **2011**, *11*, 3190.
[27] T. Szabó, O. Berkesi, P. Forgo, K. Josepovits, Y. Sanakis, D. Petridis, I. Dekany, *Chem. Mater.* **2006**, *18*, 2740.
[28] a) J. Breu, W. Seidl, A. Stoll, *Z. Anorg. Allg. Chem.* **2003**, *629*, 503; b) A. V. Talyzin, V. L. Solozhenko, O. O. Kurakevych, T. Szabo, I. Dekany, A. Kurnosov, V. Dmitriev, *Angew. Chem. Int. Ed.* **2008**, *47*, 8268; *Angew. Chem.* **2008**, *120*, 8392.
[29] P. Vecera, S. Eigler, M. Kolesnik-Gray, V. Krstic, A. Vierck, J. Maultzsch, R. A. Schafer, F. Hauke, A. Hirsch, *Sci. Rep.* **2017**, *7*, 45165.
[30] a) A. Lerf, H. He, M. Forster, J. Klinowski, *J. Phys. Chem. B* **1998**, *102*, 4477; b) H. He, J. Klinowski, M. Forster, A. Lerf, *Chem. Phys. Lett.* **1998**, *287*, 53; c) W. Cai, R. D. Piner, F. J. Stadermann, S. Park, M. A. Shaibat, Y. Ishii, D. Yang, A. Velamakanni, S. J. An, M. Stoller, J. An, D. Chen, R. S. Ruoff, *Science* **2008**, *321*, 1815; d) L. B. Casabianca, M. A. Shaibat, W. W. Cai, S. Park, R. Piner, R. S. Ruoff, Y. Ishii, *J. Am. Chem. Soc.* **2010**, *132*, 5672.
[31] H. Pieper, S. Chercheja, S. Eigler, C. E. Halbig, M. R. Filipovic, A. Mokhir, *Angew. Chem. Int. Ed.* **2016**, *55*, 405; *Angew. Chem.* **2016**, *128*, 413.
[32] H. Pieper, C. E. Halbig, L. Kovbasyuk, M. R. Filipovic, S. Eigler, A. Mokhir, *Chem. Eur. J.* **2016**, *22*, 15389.
[33] C. E. Halbig, R. Lasch, J. Krull, A. S. Pirzer, Z. Wang, J. N. Kirchhof, K. I. Bolotin, M. R. Heinrich, S. Eigler, *Angew. Chem. Int. Ed.* **2019**, *58*, 3599; *Angew. Chem.* **2019**, *131*, 3637.

Manuscript received: March 29, 2019
Accepted manuscript online: April 30, 2019
Version of record online: June 6, 2019